A comparative study of the energetics of CO on stepped and kinked Cu surfaces using density functional theory

Faisal Mehmood[1], Abdelkader Kara[1], Talat S. Rahman[1] and Klaus Peter Bohnen[2]

[1]116 Cardwell Hall, Department of Physics,

Kansas State University, Manhattan, Kansas 66506-2600, USA

[2]Forschungszentrum Karlsruhe, Institut fuer Festkoerperphysik, D-76021 Karlsruhe, Germany

(Dated: November 15, 2018)

Our *ab initio* calculations of CO adsorption on several low and high Miller index surfaces of Cu show that the adsorption energy increases as the coordination of the adsorption site decreases from 9 to 6, in qualitative agreement with experimental observations. On each surface the adsorption energy is also found to decrease with increase in coverage, although the decrement is not uniform. Calculated vibrational properties show an increase in the frequency of the metal-C mode with decrease in coordination, whereas no such effect is found for the frequency of the CO stretch mode. Examination of the surface electronic structure shows a strong local effect of CO adsorption on the local density of state of the substrate atoms. We also provide some energetics of CO diffusion on Cu(111) and Cu(211).

PACS numbers: 73.20.—r

I.   INTRODUCTION

Investigation of CO adsorption on well-defined transition metal surfaces has been of great academic interest for several decades [1, 2, 3, 4, 5, 6, 7] because of the molecule's obvious relevance to many industrial processes and as a prototype reactant in studies aiming to provide an understanding of catalytic reactions [3, 4, 5]. These experimental and theoretical [6, 7] studies have considered the importance of identifications of 'active sites' based on examination of adsorption and desorption energies and sticking coefficients [3, 4, 5]. Since real catalysts consist of small metal clusters with microfacets of various orientations, the catalyst surface is generally far from that of one with a low Miller index, rather it contains defects like steps and kinks which may play specific roles in determining its reactivity [8]. A

plausible way to understand systematically the effect of steps and kinks on chemisorption is to undertake the examination of CO adsorption on a set of vicinal surfaces, as has been done in a recent thermal deposition spectroscopy (TDS) study on Cu surfaces. These experimental studies find a dependence of the CO binding energy on the coordination of the adsorption site, but surprisingly the effect does not extend to the least undercoordinated sites, namely that of CO on the kink-sites on Cu(532). Vollmer *et. al.* [9] find hardly any difference in the adsorption energy for CO on a step and a kink site atom implying that coordination alone may not account for the adsorption energy on this vicinal surface. As proposed by Bagus *et. al.* [10] in their study of CO adsorption on Cu(100), the repulsive interaction between the O atom and the s states of the substrate can also play an important role in determining the trends in the adsorption energy. Similarly in the extensive study of CO adsorption on the (111) surface of several transition metals, Gajdos *et. al.* [11] argue that the extent of the shift of the 4σ and 5σ orbital charge density from the C-O bond to the region below the carbon (metal surface) may control the adsorption energetics. Of course, an in-depth understanding of the effect of the local electronic and geometric structure on CO adsorption may be obtained from the application of established theoretical methods such as those based on density functional theory [12, 13] to the set of Cu surfaces studied in these experiments. Such calculations may raise some concerns since on the low Miller index surfaces of Cu they have been found to: a) show preference for the hollow site [14], while the top site is preferred in the analysis of experimental data [9]; b) overestimates the CO adsorption energy [11, 14]. Very recently several groups [14, 15, 16] have attempted to supplement DFT functionals in various ways so as to remedy the two above shortcomings of DFT for this system with some success. Our intention in this paper is, however, to carry out a systematic, comparative study of CO chemisorption on the on-top sites of a set of low and high Miller index surfaces of Cu to see the trends in adsorption energies as a function of local coordination and CO coverage. While these calculations have been motivated by experimental data [9], we are also aware of theoretical work [10, 11, 15] on CO adsorption on a few of the surfaces that we are considering here. Naturally, we will compare our results to all available information that exists to date. In addition to the trends in CO adsorption energy on Cu surfaces, we are also interested in the diffusion barrier for CO, since this is a necessary step in any chemical reaction on the surface. A comparative study of the diffusion of CO on Cu(111) and Cu(211) is thus presented. Also, given the interest in reactions at and

near steps and kinks on surfaces we have carried out an examination of CO on several sites near these defects. We are also including in this work the effect of CO adsorption on the nature of atomic relaxations of the vicinal surface, to see how the trends in the relaxation patterns correlate with those in the surface electronic structure.

After giving the computational details of our work in next section, we present a detailed analysis of the calculated CO adsorption energies as a function of local coordination and their comparison to experiments and other calculations. This is followed by investigations of the implication of increasing CO coverage on adsorption energetics. Rest of the paper is devoted to the characterization of the changes in the surface electronic structure (local density of states, workfunctions) on CO adsorption. The vibrational frequencies of CO are also presented on the set of surfaces.

II.   COMPUTATIONAL METHODS

Ab initio calculations performed in this study are based on the well-known density functional theory (DFT) [12, 13]. For purposes here, a systematic study of the energetics and the electronic structure of a set of Cu surfaces of varying geometry was made by solving Kohn-Sham equations in plane-wave basis set using the Vienna *ab initio* simulation package (VASP) [17, 18, 19]. The electron-ion interactions for C, O and Cu are described by ultrasoft pseudopotentials proposed by Vanderbilt [20]. A plane-wave energy cut-off of 400 eV was used for all calculations and is found to be sufficient for these systems [11, 21]. In all calculations reported in this article, the generalized gradient correction of Perdew and Wang [22] (PW91) was used since it has been shown to give results for adsorption energetics and structural parameters which are in better agreement with experiment as compared to those obtained using the local density approximation (LDA) [14, 23]. The calculated bulk lattice constant for Cu was found to be 3.6471 Å and the Brillouin zone sampling of the total energy was based on the technique devised by Monkhorst and Pack [24] for all bulk calculations with a k-point mesh of $10 \times 10 \times 10$.

The supercell approach with periodic boundaries is employed to model the surface systems. To calculate the total energies for several coverages of CO, we have used surface unit cells consisting of $2 - 8$ atoms per layer. While the definition of the coverage for the low Miller index surfaces is conceptually easy and simply defined as the ratio of number of

adsorbate and substrate atoms in the surface unit cell, for surfaces with steps and kinks we need also to take into account the specific areas of the unit cells, for consistency. For vicinal surface we have thus adopted a definition for the coverage (θ^{vic}) which is related to the one on the (111) surface (θ) according to : $\theta^{\mathrm{vic}} = \theta \frac{A_{(111)}}{A_{\mathrm{vic}}}$, where $A_{(111)}$ is the area of the surface unit cell of Cu(111) and A_{vic} is the area of the vicinal surface. We have used 2.579 Å as the nearest neighbor distance for evaluating the area of the surface unit cell.

Cu(100) and Cu(111) surface systems were modeled by a 4 layer (16 atoms) tetragonal and hexagonal supercell, respectively. These 4 layers are separated with 11 Å of vacuum. For Cu(100), calculations were performed for $c(2 \times 2)$ overlayer corresponding to 50% coverage of CO and for a (1×1) structure corresponding to full coverage even though such a high coverage is unrealistic. For Cu(111), the $p(2 \times 2)$ structure corresponding to 33% CO coverage, and those corresponding to coverages of 66% and 100% were also studied. For all coverages considered on Cu(100) and Cu(111), the CO molecule was taken to be adsorbed on the on-top sites, with the molecule sitting perpendicular to the surface and the C atom forming a bond with the Cu surface, as also reported in number of experiments [9, 25, 26]. A $4 \times 4 \times 1$ Monkhorst-Pack k-point mesh was used for Cu(100) and of $5 \times 5 \times 1$ for Cu(111).

The Cu(110), Cu(211) and Cu(221) surfaces were modeled by an orthorhombic supercell of 8, 17 and 22 layers, respectively, separated with approximately 12 Å vacuum. For Cu(110), a (2×1) surface unit cell (16 Cu atoms) with 1 and 2 CO molecules were chosen to model 50% and 100% coverage of CO, respectively, as shown in the Fig. 1c. A Monkhorst-Pack k-point mesh of $5 \times 7 \times 1$ was used for this surface. Both Cu(211) and Cu(221) being regularly stepped surfaces with monoatomic steps and terrace width of 3 and 4 atoms, needed 34 and 44 atoms, respectively, to model a (2×1) surface unit cell. For Cu(211), this supercell corresponds to 17.69% coverage, while for Cu(221) the corresponding coverage is 14.44%. Calculations for twice the coverage were also performed by incorporating an additional CO molecule in the same supercell. The detailed analysis was performed for the on-top and the bridge site, also for Cu(221), for which the (2×1) supercell corresponds to 14.44% CO coverage and an additional atom in the same supercell boosts the coverage to 28.88%. A Monkhorst-Pack k-point mesh of $5 \times 4 \times 1$ was used for (211) and $5 \times 3 \times 1$ was used for the (221) surface. Finally, Cu(532) whose surface consists of regularly spaced kinks, was modeled by a simple monoclinic supercell of five layers, where each layer has 8 non-equivalent atoms. These five layers were separated with 12 Å of vacuum. A Monkhorst-Pack k-point

mesh of $3 \times 4 \times 1$ was used and CO was adsorbed on top of the Cu atom at the kink site which is the experimentally proposed preferred site [9]. Two coverages (10.76% and 21.52%) of CO on Cu(532) were modeled by adsorbing one and two molecules, respectively, on the kink site (and on a site very next to kinked site).

Since vicinal surfaces provide local environments with a range of coordinations and a hierarchy of adsorption sites may exist on them [27], we have carried out calculations for one of the stepped surfaces, Cu(211), for eight different sites as indicated in Fig. 1d. Since these results point to a preference for the bridge site, for Cu(221) and Cu(532) we have calculated adsorption energies for the bridge sites, in addition to the on-top site.

In order to calculate the total energy of the system for a relaxed configuration, atoms on all surfaces considered were allowed to move in all three directions and the structures were relaxed until the forces acting on each atom were converged to better that 0.02 eV/Å. The adsorption energies were calculated by subtracting the total energy of the CO-molecule and that of the corresponding fully relaxed clean-Cu surface system from the total energy of CO/Cu surface system $E_{ad} = E_{CO/Cu} - E_{CO} - E_{Cu}$. Another quantity of interest, the workfunction, was calculated by taking the difference of the average vacuum potential and Fermi energy for each surface. Finite difference method was used to obtain vibrational frequencies of the CO molecule in the gas phase and on the surfaces. CO internal stretching and CO-metal stretch frequencies were calculated in the direction perpendicular to the surface. To analyze the nature of the bonding between CO and the Cu-atoms, local density of states were also obtained. A Gaussian function of 0.2 eV width was used to smoothen the local density of states (LDOS).

III.   RESULTS AND DISCUSSION

As already mentioned above, the collection of surfaces studied here provide variation of adsorption sites with coordination ranging from 6 to 9. The kink sites with coordination 6 on Cu(532) are particularly interesting because of their unexpected results from TDS measurements [9]. Also of significance is the fact that the step edges of Cu(211) and Cu(221) represent the two different microfacets of monoatomic steps on fcc(111) surfaces. Cu(211) has the (100)-microfacet while Cu(221) has the (111)-microfacet. It will be interesting to see if such differences in their geometry affect the energetics of CO on these surfaces. In Table

I, we have compared our calculated CO bond length and the corresponding surface-carbon distance for these three surfaces. While the C-O bond length remains insensitive to the local geometry and coordination, C-Cu bond is much shorter for bridge (b) then ontop (t) site adsorption. As for Cu(532) there are two non equivalent bridge sites labeled by b_{KS1} and b_{KS2} in Table I and Fig. 1f. The C-O bond lengths are very close to the ones calculated by others [25, 26]. When CO is adsorbed on the bridge site on the three vicinal surfaces, the CO bond length slightly increases and the carbon-surface distance decreases. Earlier DFT calculations for CO on Cu(211) also find the same trend [21]. The only available date [28, 29, 30] of bond lengths is for the low Miller index surfaces and is in good agreement with our calculated value of 1.16 Å for the C-O bond length and 1.85 Å and 1.86 Å C-Cu bond for Cu(111) and Cu(100), respectively. When compared to vicinal surfaces, we do not see any difference for C-O bond length and a small variation within 0.02 Å for C-Cu bonds. A small increase of 0.02 Å was seen in C-Cu bond when CO coverage was increased from 33% to 100% whereas when coverage is doubled from 50% in Cu(100) and Cu(110), we see only 0.01 Å increase in C-Cu bonds and no change was found in C-O bond lengths.

A. Adsorption Energies

Our calculated CO adsorption energies on various Cu surfaces and their surface atomic coordination is summarized in Table II. The lowest coordinated and in turn the most favorable for CO adsorption is the kink atom on Cu(532) (Fig. 1f), with the highest adsorption energy of 0.98 eV at a coverage of 10.75% CO (i.e. one CO molecule/per kink atom). The calculated adsorption energy for this case is found to be particularly higher than what has been seen experimentally. Although overestimation of adsorption energies is typical of DFT based calculations, it is expected that the qualitative behavior would be similar. For CO adsorption on the steps of Cu(110), Cu(211) and Cu(221) with atomic coordination 7, our calculations find E_{ad} to be about 0.86 ± 0.01 eV, while experimental values are around 0.6 eV. For adsorption on the kink site we predict an increase in E_{ad} while experiments [9] find it to be same as for the steps. As is clear from Fig. 2 our calculated values scale nicely with the surface coordination and the variation is larger than that extracted from experimental data, which is plotted in Fig. 2 for comparison. The natural question is why this difference between theory and experiment. We offer here a few rationale. For example, there

is the possibility that site blocking by another CO could lead to smaller measured value on an open surface like Cu(532). To test the viability of this proposition, we adsorbed an additional CO molecule on a site next to the kink site (SC1 in Fig. 1f) which increased the coverage to 21.5%. As we see in Table II, this leads to a decrease in the adsorption energy to 0.85 eV which is very close to what we find for Cu stepped surfaces. The variation of the adsorption energy with coverage is quite remarkable for all surfaces considered. For Cu(221) E_{ad} changes from 0.85 eV for 14.5% coverage to 0.65 for 29% coverage. Although DFT studies of CO adsorption on Cu(110) and Cu(211) have already been reported in the literature [11, 15, 21, 31], for consistency we have included them in Table II. Though we have used the same (2×1) cell for Cu(211), this leads to a different coverage (17.69%) from that on Cu(221) because of the difference in the terrace width. The same (2×1) cell used for Cu(110) (with [110] being x and [100] being y-directions), as shown in Fig. 1c, results in a 50% coverage. The CO molecule is adsorbed on the top site on Cu(110) and Cu(211), as shown in Fig. 1d and 1e. Our calculated adsorption energies are within 20 meV of each other for all of cases involving atoms with coordination 7. For Cu(211) our calculated value is somewhat smaller than in Ref. [11] which may be associated with the differences in calculational details. For CO adsorption on Cu(110) Liem *et. al.* [31] obtained an adsorption energy of 0.95 eV for the same coverage and on-top site. The discrepancy with our results could be due to the usage of fewer layers and smaller k-point mesh and energy cut-off in their calculations. For example, we find the adsorption energy to change from 0.87 eV to 0.89 eV when we reduce the number of layers in our supercell from 8 to 6 (note that a three layer slab was used in Ref. [31]). Also, we have found an energy cut-off of 300 eV to be not sufficient to provide converged results for the total energy for open surfaces such as the (110). A cut-off of at least 400 eV (value used in all our calculations) is required for accurate determination of adsorption energies.

For the next surface in this hierarchy Cu(100) whose surface atoms have coordination 8, we obtain an adsorption energy of 0.77 eV for a 50% CO coverage. This result is again higher than the experimental value which ranges, between 0.5 and 0.57 eV [26, 32]. On the other hand, our result is close agreement with the calculated value of 0.863 eV found for a smaller coverage of 0.25 ML by Gajdos and Hafner [15], using the same DFT technique. Finally, we turn to Cu(111) which has a surface atoms with coordination 9 and displays the lowest adsorption energy of all surfaces discussed here. For this particular surface, we have

used the experimentally studied $p(2 \times 2)$ overlayer which corresponds to 33% CO coverage. For 0.25 ML coverage an adsorption energy of 0.74 eV has already been reported [11]. The small difference from our result of 0.634 eV may be assigned to the difference in coverage, and is consistent with a decrease of adsorption energy with an increase of coverage. The clear trend of increasing adsorption energy with decreasing local coordination can be seen from the plot in Fig. 2 where solid triangles are our calculated values and empty triangles are the one from the experiment [9].

As expected we find a hierarchy of adsorption sites on Cu(211). The bridge site (labeled 2 in Fig. 1d) was found to be slightly preferred over on-top by ~ 0.06 eV. The sites labeled 3 (fcc-hollow) and 4 (hcp hollow near step edge), in Fig 1d were the next preferred with adsorption energies of 0.78 and 0.89 eV, respectively. The least favorable site on this surface was found to be the site labeled 6 which is between two step edges and two corner atoms and has highest number of bonds with the carbon atom and an adsorption energy of 0.56 eV. On Site 5, 7 and 8 adsorption energies are very close to each other ranging from 0.6 - 0.65 eV. The adsorption site with the highest coordination is the corner atom (CC) on Cu(211) with effective surface coordination of 10, and labeled as site # 8 in Fig. 1d for which we find the adsorption energy to be the lowest of all (0.617 eV), consistent with the above discussion. Note that we find the bridge site to be also preferred by about 0.08 eV over the on-top site for CO adsorption on Cu(221). On the other hand, for Cu(532) which has two non-equivalent bridge sites referred as b_{KS1} and b_{KS2} in Table II and Fig. 1f, we find the adsorption energy to be 0.94 eV which is less than that on the kink site.

In all cases, adsorption energies drop by $130 - 250$ meV when the coverage is doubled for these high Miller index surfaces. Various experiments already show the strong dependence of adsorption energy on CO coverage on Cu surface [33, 34, 35]. The electron energy loss spectroscopy (EELS) experiment of Peterson *et. al.* [34] shows a 50% decrease in adsorption energy for 0.3ML increase in CO coverage for Cu(100).

B. CO diffusion on metal surface

One of the experimental techniques to determine the adsorption energies is the temperature programmed desorption (TPD). It is hence desirable to develop a techniques by which TPD spectra are calculated for a given system. For the case of low Miller index surfaces,

the task may be trivial as only a limited number of processes are involved. But for the case of real surfaces with steps and kinks, the situation become more cumbersome. To achieve a realistic description of TPD spectra from these surfaces, one needs to calculate not only adsorption energies for sites with different local environments, but also activation energies associated with different diffusion paths. As we have reported above, the CO molecules adsorb preferably near kinks and steps, and it is hence rarely that CO molecules sit on the down side of the terrace (sites 6 and 8 in Fig. 1d). The relevant energies are hence those associated with diffusion on Cu(111) and near the step of a Cu vicinal surface. Here we have in mind systems dominated by the presence of (111) facets and step edges. The knowledge of these activation energies along with the different adsorption energies will constitute the base for kinetic Monte Carlo simulations that will determine the TPD spectra. In order to reach this goal, the energy landscape for the diffusion of CO on Cu(111) and Cu(211) surfaces were calculated. Since we were interested in describing the motion of the CO molecule between the equilibrium sites, the path on Cu(111) was chosen to be from one top site to the adjacent one, passing through fcc-hollow, bridge, and hcp hollow sites (Fig. 3). All layers of the metal surface, and C and O atoms were allowed to relax fully in all three directions on high symmetry sites. For the intermediate sites only carbon atom was fixed in one direction and rest of the system was allowed to relax fully. Three intermediate points between the top and the bridge site and two points for each bridge - fcc-hollow and bridge - hcp-hollow were calculated, as shown in Fig.4a. The relative energy profile of the CO molecule on Cu(111) is shown in Fig. 4a. As in previous studies, our calculations based on DFT with GGA indicate that CO prefers to sit on fcc hollow site instead of the top site. However, our calculations show a barrier of about 200 meV to go from the hollow to the top site and less than 100 meV to go from the hollow to the bridge site. Fig. 4b and 4c, show the one dimensional energy landscape for the CO molecule on Cu(211). Two diffusion paths are chosen in this case: a) top - bridge - top (along the step edge) and b) top - fcc-hollow (away from the step). Fig. 4b indicates that diffusion from bridge to top is more favorable than from top to hollow with diffusion barrier about 60 meV compared about 200 meV barrier for diffusion from top to hollow site. These results indicate that CO molecules are more free to roam on the step edge of Cu(211) than away from it.

C. Interlayer Relaxations

In Table III, we present a comparison of the interlayer relaxations of the stepped and kinked Cu surfaces as introduced by the adsorption of the CO molecule. The results for the corresponding clean surfaces are also included. The Cu(532) surface has the most dramatic effect of CO adsorption as $d_{1,2}$ is found to have a large outward relaxation of $+23.5\%$ compared to an inward relaxation of -17.7% for the clean surface. The effect is local and as seen from Table III, there is only a small change in the relaxations for the rest of the layers on CO adsorption. There is so far no experimental data available for interlayer relaxation on Cu(532), however, our calculated trend for clean Cu(532) is in agreement with those calculated with many body potentials [36]. On the stepped surface Cu(221), the effect of CO adsorption is also mostly on $d_{1,2}$ in which large inward relaxation of -16.5% on the clean surface is overtaken by a small outward relaxation of $+2.9\%$. Calculated interlayer relaxation on clean Cu(221) matches well with those obtained with the full-potential linear augmented plane-wave method (FPLAPW) [37] and many body potentials [38] for this surface. The interlayer relaxations of clean Cu(211) agrees with those obtained from low energy electron diffraction measurements and previous theoretical techniques [21, 39, 40]. Like other two surfaces, Cu(211) shows that the strong contraction of -15.6% between layer 1 and 2 ($d_{1,2}$) of the clean surface is overtaken by a small inward relaxation of $+6.4\%$ on CO chemisorption.. This general trend of the change in the top layer relaxation from a large contraction to expansion upon adsorption of CO is in well accord with the observation by Ibach and Bruchman [41] who reported a surface vibrational mode above the bulk band for the vicinal surface Pt(775) (due to the large contraction) that disappears when CO is adsorbed (reflecting the change of the large contraction to an expansion).

D. Vibrational Properties and Workfunctions

Vibrational properties of a 'free' CO molecule were calculated by fully relaxing a single molecule in a large super cell of size, approximately $6 \times 6 \times 22$ Å. The stretching mode was calculated to be 264.5 meV. This can be compared with the experimentally measured frequency of isolated CO molecule of 257.8 meV with EELS and of 257.7 meV with infrared (IR) spectroscopy [42, 43]. For CO-covered Cu surfaces, we have calculated the frequencies

of two modes: the metal - molecule (ν_{C-Cu}) stretch and the intra-molecular stretch (ν_{C-O}). We find a small drop in the vibrational frequency as compared to that of the gas phase CO due to the bonding on CO with the Cu surface atom. The frequencies of the CO vibrational modes calculated for all surfaces are summarized in Table IV. For all cases in which CO is adsorbed on the top site we see almost the same value of the CO stretching frequency (ν_{C-O}), as expected. However, there is a small increase in (ν_{C-Cu}), with a decrease in the coordination of the substrate atom. This is also to be expected since molecules adsorbed on low coordinated sites will have stiffer bonds than those on highly coordinated sites. Whereas, for the case of the bridge site, there is a decrease of approximately $14-16$ meV in CO stretch frequency, from that for top site, for all cases. In this case understood due to the molecule strongly bonded with two surface atoms and being not as free to vibrate as on top site. The drop in ν_{C-Cu} mode is also $2-4$ meV greater than top site.

In Table V, we have summarized the calculated workfunctions for all Cu surfaces considered here, with and without the adsorbate along with available experimental values for clean surfaces of Cu(100), Cu(111) and Cu(110). Our calculated workfunctions are smaller than the experimental values of the known surfaces [44, 45, 46]. Our calculated values showed a decrease in workfunctions for clean surfaces with decrease in coordination of substrate. A similar kind of behavior can be seen in the experiments for (111), (100) and (110) surface [44, 45, 46]. Our calculations also showed an increasing trend on workfunction when CO is adsorbed on the surface. This effect is strongest for Cu(100) surface with workfunction change of 0.57 eV for all other surfaces this change is less than 0.17 eV.

E.   Surface Electronic Structure

When an electronegative element like C is adsorbed on a metallic surface, it tends to take charges away from the surface. This would have a strong dependence upon the coordination of the adsorbate as reported in many studies [47]. Since we have considered CO adsorption on a variety of local atomic environments it is important that we examine the differences in the local electronic structure and the nature of the bonding of the CO with the substrate. In Fig. 5 - Fig. 7, we have plotted the local density of d-state (LDOS) of Cu atoms and sp-states for C and O atoms to study the sp-d hybridization, for three high Miller index surfaces of interest here. First of all, we see narrowing (Fig. 5 - Fig. 7) of the d-band for

the lower coordinated surfaces, as seen by Tersoff *et. al.* [48] for their calculations of Ni and Cu surfaces. The *sp*-state of C and O are split and have almost filled bonding band. These states make sub-bands with *d*-state of Cu surface in all case which can be seen to appear at the same low energies as for CO case. This affect is found to be more localized on flat surfaces but on stepped surfaces, even though CO is adsorbed on top site we see a small change in redistribution of LDOS for next layer atom, which can be caused due to the small inter layer separation i.e. 0.296 Å for (532) as compared to the biggest 2.1 Å for (111) case. The next layer atom being so close to CO also experiences some affect of the adsorbate. This could well describe the different adsorption energies with different coordination. Along with this electronic charge density distribution and LDOS for these atoms we can safely say that this difference for flat (high coordinated sites) and stepped and kinked (low coordinated sites) could serve as the basis of different adsorption energies.

IV. CONCLUSIONS

In this paper, we have presented the results of a detailed theoretical investigation of CO adsorption on three low Miller index surfaces, namely, (111), (100), (110), two stepped surfaces, (211) and (221), and a kinked (532) surface of Cu. The CO was adsorbed on experimentally observed preferred sites to explain trends in adsorption energies due to different geometrical and chemical structure. Our calculated values of adsorption energies show the increasing trend with decrease in local coordination of surface atoms with Cu(532) being the most favorable surface for CO adsorption with lowest coordination. However bridge sites of Cu(211) and Cu(221) were found to be slightly preferred over top site which was not the case for Cu(532). We also found a strong dependence of adsorption energy on coverage of the adsorbate. Our calculations show a large decrease in adsorption energy with increase in coverage. Our calculations of diffusion of CO molecule on metal surfaces indicate that it diffuses much more easily along the step edge as compared to away from the step edge (terrace). A very small drop in vibrational frequency of free molecule was noted when it was adsorbed on the metal surface but difference within different surfaces was negligible due to same on top adsorption site for all surfaces. Workfunction of adsorbate covered surface was found to increase in all cases compared to the clean surface.

Acknowledgments

---

[1] G. Blyholder, J. Phys. Chem. **68**, 2772 (1964).

[2] P. S. Bagus, C. J. Nelin and C. W. Bauschlicher, Phys. Rev. B **28**, 5423 (1983).

[3] S. M. Davis and G. A. Somorjai, in The Chemical Physics of Solid Surfaces, edited by D. A. King and D. A. Woodruff (Elsevier, Amsterdam, 1982), Vol. 4.

[4] J. C. Campazona, in The Chemical Properties of Solid Surfaces and Heterogenous Catalysis, edited by D. A. King and D. P. Woodruff (Elsevier, Amsterdam, 1990), Vol. 3, Part A.

[5] H. Wagner, in Springer Tracts in Modern Physics, edited by G. Hoehler (Springer, Berlin, 1987).

[6] H. Over, Prog. Surf. Sci. **58**, 249 (2001).

[7] S. Sung and R. Hoffmann, J. Am. Chem. Soc. **107**, 578 (1985).

[8] C. R. Henry, Surf. Sci. Rep. **31**, 231 (1998).

[9] S. Vollmer, G. Witte, C. Wöll, Cat. Lett., **77**, 97 (2001).

[10] P. Bagus and C. Wöll, Chem. Phys. Lett. **294**, 599 (1999).

[11] M. Gajdos, A Eichler, and J. Hafner, J. Phys.: Condens. Matter. **16**, 1141 (2004).

[12] P. Hohenberg and W. Kohn, Phys. Rev. **136**, 864 (1964).

[13] W. Kohn and L. J. Sham, Phys. Rev. **140**, A1133 (1965).

[14] F. Favot, A. D. Corso, and A. Baldereschi, J. Chem. Phys. **114**, 483 (2001).

[15] M. Gajdos and J. Hafner, Surf. Sci., **590**, 117 (2005).

[16] S. E. Mason, I. Grinberg, and A. M. Rappe, Phys. Rev. B **69**, 161401 (2004).

[17] G. Kresse and J. Hafner, Phys. Rev. B **47**, 558 (1993).

[18] G. Kresse and J. Furthmuller, Comput. Mater. Sci. **6**, 15 (1996).

[19] G. Kresse and J. Furthmueller, Phys. Rev. B **54**, 11169 (1996).

[20] D. Vanderbilt, Phys. Rev. B. **41**, 7892 (1990).

[21] M. Gajdos, A. Eichler, J. Hafner, G. Meyer, and K-H Rieder, Phys. Rev. B. **71**, 035402 (2005).

[22] J. P. Perdew, J. A. Chevary, S. H. Vosko et al., Phys. Rev. B **46**, 6671 (1992).

[23] P. Fouquet, R. A. Olsen, and E. J. Baerends, J. Chem. Phys. **119**, 509 (2003).

[24] H. J. Monkhorst and J. D. Pack, Phys. Rev. B **13**, 5188 (1976).

[25] J. Braun, A. P. Graham, F. Hofmann, W. Silvestri, J. P. Toennies, and G. Witte, J. Chem. Phys., **105**, 3258 (1996).

[26] A. P. Graham, F. Hofmann, J. P. Toennies, G. P. Williams, C. J. Hirschmugl, and J. Ellis, J. Chem. Phys. **108**, 7825 (1998).

[27] S. Stolbov, F. Mehmood, T. S. Rahman, M. Alatalo, I. Makkonen, and P. Salo, Phys. Rev. B **70**, 155410 (2004).

[28] E. J. Moler, S. A. Kellar, W. R. A. Huff, Z. Hussain, Y. Chen, and D. A. Shirley, Phys. Rev. B **54**, 10862 (1996).

[29] S. Andersson and J. B. Pendry, Phys. Rev. Lett. **43**, 363366 (1979).

[30] C. F. McConville, D. P. Woodruff, K. C. Prince, G. Paolucci, V. Chab, M. Surman, and A. M. Bradshaw, Surf. Sci. **166**, 221 (1986).

[31] S. Y. Liem and J. H. R. Clarke, J. Chem. Phys. **121**, 4339 (2004).

[32] A. Föhlisch, W. Wurth, M. Stichler, C. Keller, and A. Nilsson, J. Chem. Phys. **121**, 4848 (2004).

[33] J. C. Tracy, J. Chem. Phys. **56**, 2748 (1972).

[34] L. D. Peterson and S. D. Kevan, Surf. Sci. Lett. **235**, L285 (1990).

[35] C. M. Truong, J. A. Rodriguez, and D. W. Goodman, Surf. Sci. Lett. **271**, L385 (1992).

[36] F. Mehmood, A. Kara, T. S. Rahman, to be published.

[37] J. L. F. Da Silva, K. Schroeder, and S. Blügel, Phys. Rev. B **70**, 245432 (2004).

[38] I. Y. Sklyadneva, G. G. Rusina, and E. V. Chulkov, Surf. Sci. **416**, 17 (1998).

[39] S. Durukanoğlu, A. Kara, and T. S. Rahman, Phys. Rev. B **55**, 13894 (1997).

[40] T. Seyller, R. D. Diehl, and F. Jona, J. Vac. Sci. Technol. A **17**, 1635 (1999).

[41] H. Ibach and D. Bruchmann, Phys. Rev. Lett. **41**, 958 (1978).

[42] C. J. Hirschmugl, G. P. Williams, F. M. Hoffmann, and Y. J. Chabal, Phys. Rev. Lett. **65**, 480 (1990).

[43] R. Raval, S.F. Parker, M.E. Pemble, P. Hollins, J. Pritchard, and M.A. Chesters, Surf. Sci. **203**, 353 (1988).

[44] C. J. Fall, N. Binggeli, and A. Baldereschi, Phys. Rev. B **61**, 8489 (2000).

[45] R. Arafune, K. Hayashi, S. Ueda, and S. Ushioda, Phys. Rev. Lett. **92**, 247601 (2004).

[46] W. Mantz, James K. G. Watson, K. Narahari Rao, D. L. Albritton, A. L. Schmeltekopf, and R. N. Zare, J. Mol. Spectrosc. **39**, 180 (1971).

[47] A. Föhlisch, M. Nyberg, J. Hasselström, O. Karis, L. G. M. Pettersson, and A. Nilsson, Phys. Rev. Lett. **85**, 3309 (2000).

[48] J. Tersoff and L. M. Falicov, Phys. Rev. B **24**, 754 (1981).

TABLE I: Calculated structural properties of CO adsorbed on the top (t) and bridge (b) sites on Cu(211), Cu(221) and Cu(532). The two non equivalent bridge sites on Cu(532) (see Fig. 1f) are labeled as b_{KS1} and b_{KS1}. Values in square brackets are reported by others [21].

Surface	Bond Lengths (Å)	
	d_{C-O}	d_{C-Cu}
Cu(211)	1.16 (t)[1.154]	1.85 (t)[1.84]
	1.17 (b)[1.168]	1.51(b)[1.50]
Cu(221)	1.16 (t)	1.86 (t)
	1.17 (b)	1.51 (b)
Cu(532)	1.16 (t)	1.85 (t)
	1.17 (b_{KS1})	1.56 (b_{KS1})
	1.17 (b_{KS2})	1.58 (b_{KS2})

TABLE II: Variation of the adsorption energies (E_{ad}) of CO for two coverages on several Cu surfaces. The coverage in the lower entry (in parenthesis) is twice as large as the one for the top entry for each surface. In the upper entries the experimental values from Ref [9] are in parenthesis. N_{NN} is the coordination of the adsorption site.

Surface	Cu(111)	Cu(100)	Cu(110)	Cu(211)	Cu(221)	Cu(532)
N_{NN}	9	8	7	7	7	6
E_{ad} (eV)	0.634(0.49)	0.77(0.53)	0.87(0.56)	0.86(0.61)	0.85(0.60)	0.98(0.59)
				0.925(b)	0.933 (b)	0.941(b_{KS1})
						0.949(b_{KS2})
	0.18(100%)	0.18(100%)	0.55(100%)	0.61(35.4%)	0.65(28.9%)	0.85(21.5%)

TABLE III: Comparison of clean and CO covered % multilayer relaxations.

$d_{i,i+1}$	Cu(211)	CO/Cu(211)	Cu(221)	CO/Cu(221)	Cu(532)	CO/Cu(532)
$d_{1,2}$	−15.6	+6.4	−16.5	+2.9	−17.7	+23.5
$d_{2,3}$	−11.4	−15.7	−1.9	−10.2	−18.9	−18.8
$d_{3,4}$	+11.3	+0.2	−15.2	−9.5	−12.7	−16.2
$d_{4,5}$	−4.1	+6.9	+18.8	+6.0	−15.0	−12.0
$d_{5,6}$	−2.0	−3.9	−2.9	+3.8	−15.0	−16.6
$d_{6,7}$	+2.0	−1.8	−6.1	−2.7	−1.4	−3.9
$d_{7,8}$	−2.1	+1.8	+2.5	+2.0	+1.9	−5.2
$d_{8,9}$	+0.1	−0.6	+2.3	−4.4	+25.0	+16.4
$d_{9,10}$			−0.9	+2.2	−9.7	+9.6
$d_{10,11}$			+2.0	+1.0	−2.9	−6.6
$d_{11,12}$			+0.8	−1.1	−4.7	−5.4
$d_{12,13}$				−0.1	−2.0	−0.6
$d_{13,14}$					+0.2	−3.3
$d_{14,15}$					−1.1	−2.9
$d_{15,16}$					+0.1	+3.7
$d_{17,18}$					+1.1	−4.2
$d_{18,19}$					−1.8	+2.3
$d_{19,20}$					−1.6	−4.8
$d_{20,21}$					−0.7	+1.1

TABLE IV: Calculated CO frequencies. ν_{C-O} is for the streching mode of the CO molecule and ν_{C-Cu} is between the surface and the CO-molecule. Here 't' and 'b' represent the top and bridge sites (see Fig. 1).

Surface	Vibrational Frequency (meV)	
	ν_{C-O}	ν_{C-Cu}
Cu(211)	251.2 (t)	40.3 (t)
	236.2 (b)	38.4 (b)
Cu(221)	251.0 (t)	40.1 (t)
	235.5 (b)	36.7 (b)
Cu(532)	252.1 (t)	41.0 (t)
	235.7 (b_{KS1})	36.0 (b_{KS1})
	233.9 (b_{KS2})	36.4 (b_{KS2})

TABLE V: Calculated workfunctions (eV) for clean Cu surface and CO adsorbed surfaces along with the available experimental values in parenthesis. The experimental values are taken from [43, 44, 45].

Surface	(111)	(100)	(110)	(211)	(221)	(532)
Clean	4.89 (4.98)	4.63 (4.65)	4.49 (4.52)	4.57	4.58	4.48
With CO	4.93	4.67	4.68	4.72	4.75	4.64
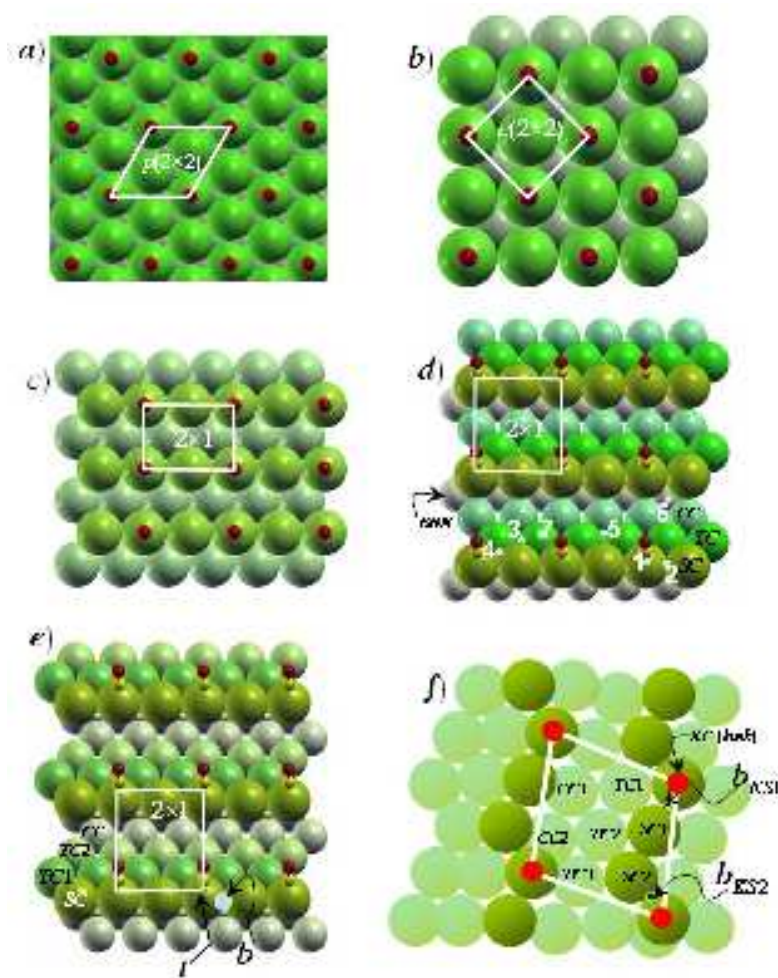
FIG. 1: Top view of a) 111, b)100, C)110, d)211, e) 221 and f) 532 surface. Different coverages at different sites are shown. Dark colors represents top layer. Note that in 532 surface all eight atoms are non-equalent and belongs to eight different layers.
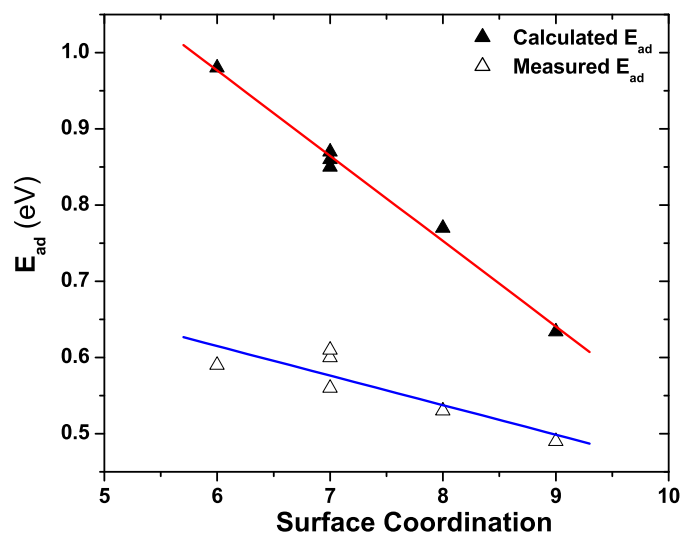
FIG. 2: Adsorption energy versus local surface coordination. Solid triangles are calculated values and empty are experimental.
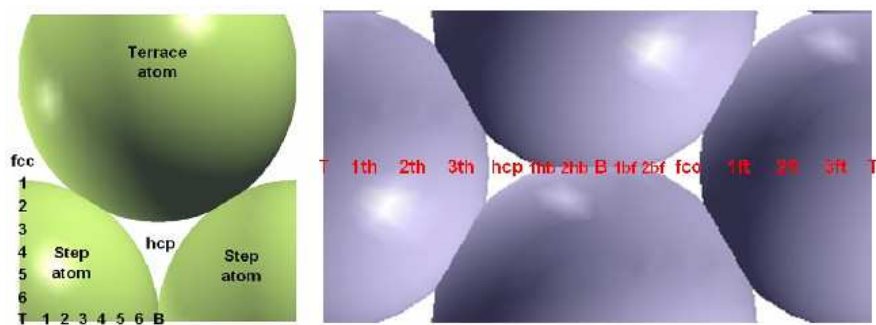
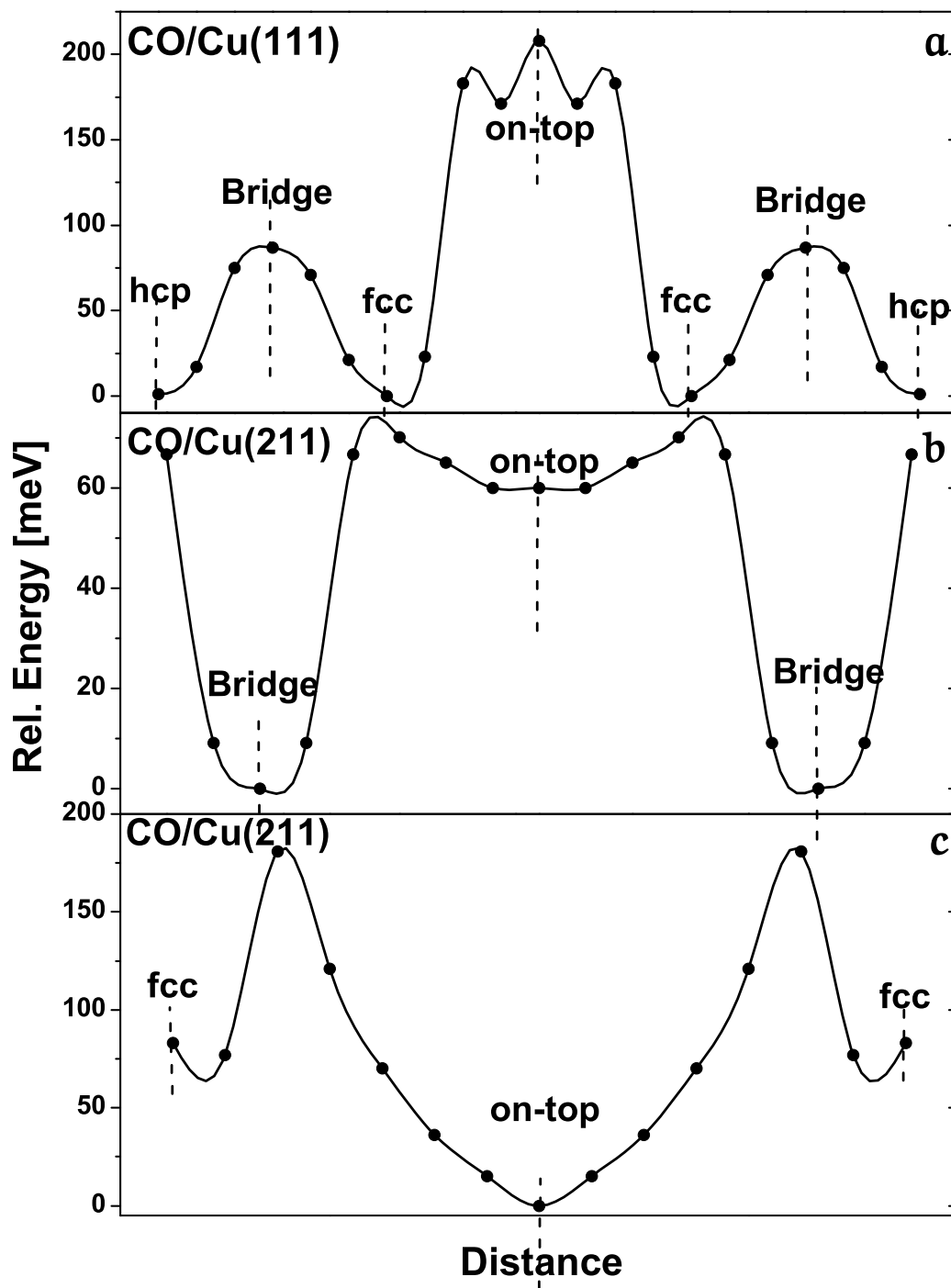FIG. 3: Chosen diffusion path for CO molecule on a) Cu(111) and b) Cu(211).

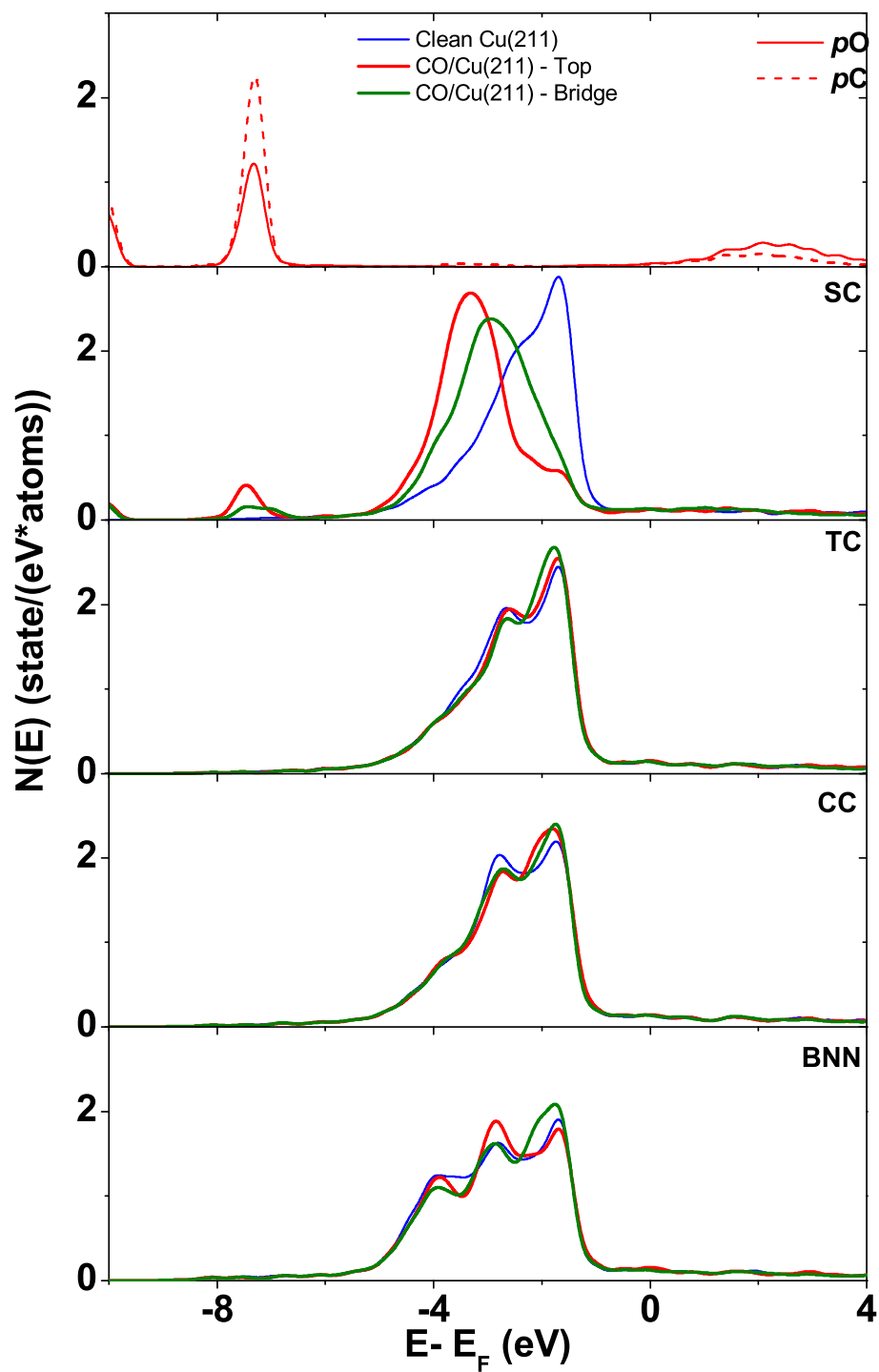
FIG. 4: Diffusion of CO molecule on a) Cu(111) and b), c) Cu(211).

FIG. 5: Local density of state of clean Cu(211) and with CO on top and bridge sites are shown in Fig. 1d.
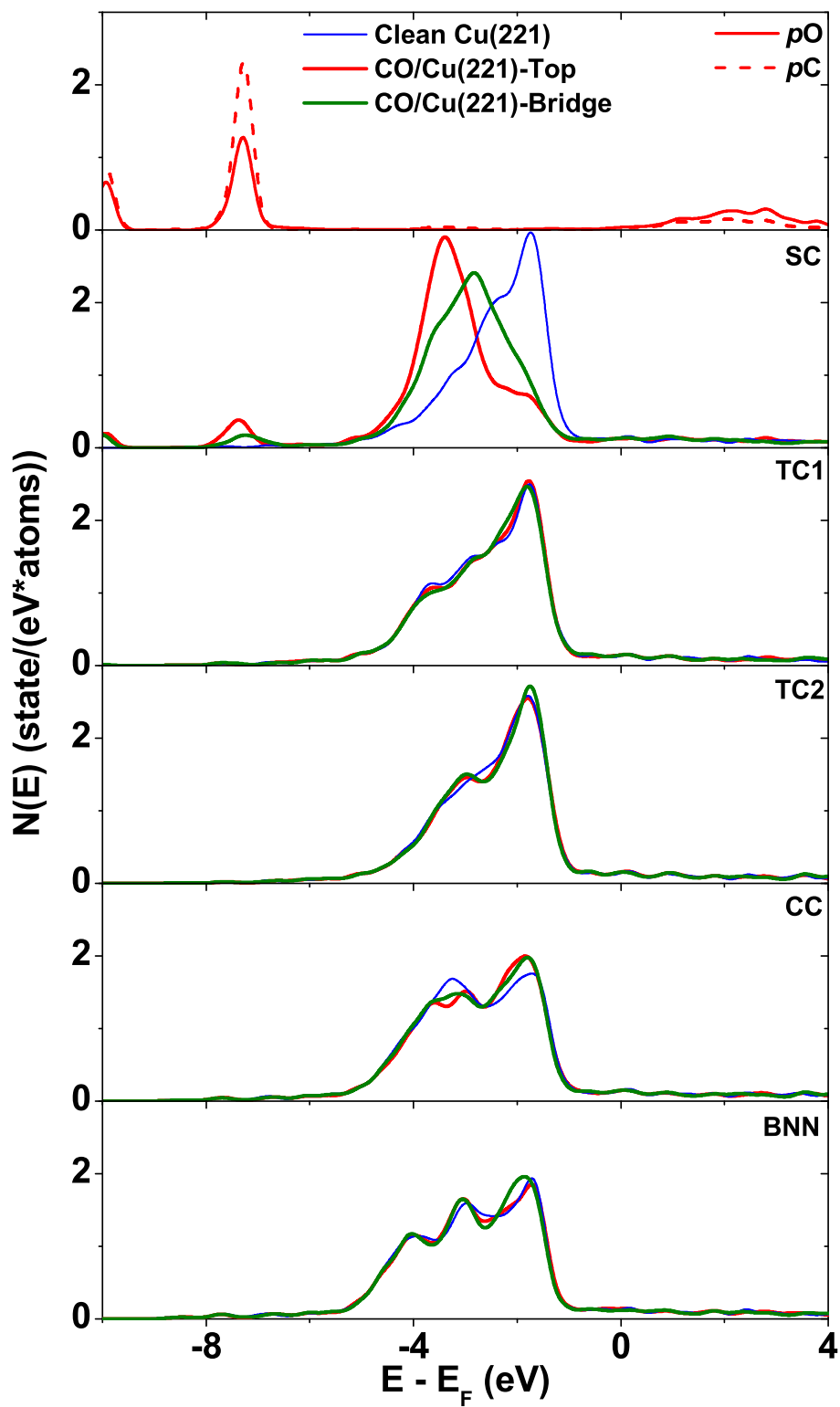
FIG. 6: Local density of state of clean Cu(221) and with CO on top and bridge sites are shown in Fig. 1e.
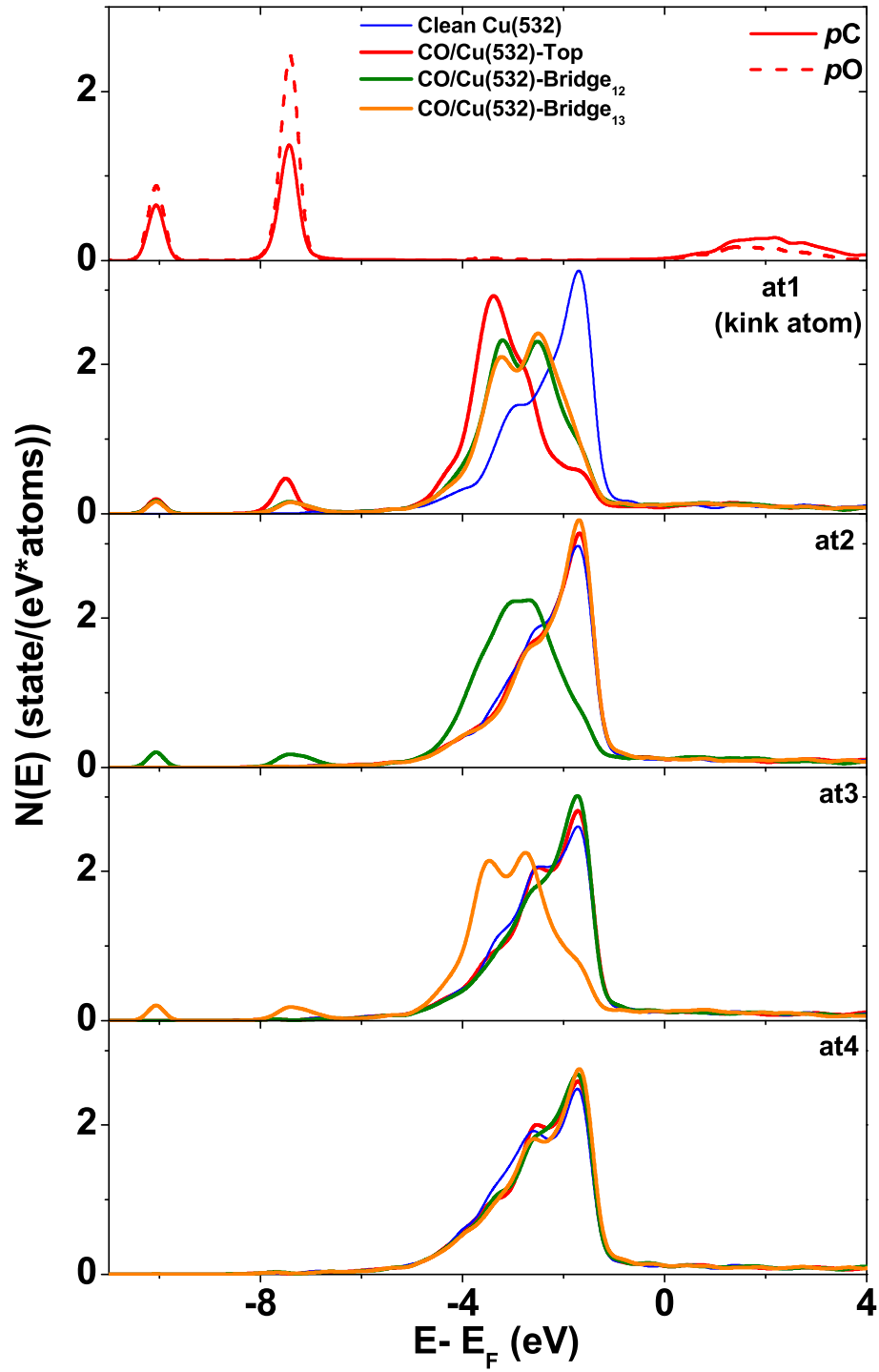
FIG. 7: Local density of state of clean Cu(532) and with CO on top (kink) and two bridge sites are shown in Fig. 1f.